

The effect of interface state continuum on the impedance spectroscopy of semiconductor heterojunctions

This content has been downloaded from IOPscience. Please scroll down to see the full text.

2013 Semicond. Sci. Technol. 28 025013

(<http://iopscience.iop.org/0268-1242/28/2/025013>)

View [the table of contents for this issue](#), or go to the [journal homepage](#) for more

Download details:

IP Address: 131.174.75.30

This content was downloaded on 09/12/2013 at 13:40

Please note that [terms and conditions apply](#).

The effect of interface state continuum on the impedance spectroscopy of semiconductor heterojunctions

V V Brus

Chernivtsi Branch, Frantsevich Institute for Problems of Materials Science of NAS of Ukraine,
58001 Chernivtsi, Ukraine

Department of Electronics and Energy Engineering, Chernivtsi National University, 58012 Chernivtsi,
Ukraine

E-mail: victorbrus@mail.ru

Received 15 September 2012, in final form 20 November 2012

Published 8 January 2013

Online at stacks.iop.org/SST/28/025013

Abstract

A quantitative analysis of the impedance spectroscopy of semiconductor heterojunctions was carried out in the presence of interface state continuum at the heterojunction interface. A comparison of the impedance spectroscopy of semiconductor heterojunctions simulated in the context of the interface state continuum model with that simulated in the scope of the single-level state model was carried and possible misinterpretations were considered. The previously proposed approaches for the determination of the interface-state-related parameters and for the calculation of the actual barrier capacitance (the single-level state model) were modified in order to take into account the effect of interface state continuum.

(Some figures may appear in colour only in the online journal)

1. Introduction

Impedance spectroscopy is a powerful tool for the investigation of semiconductor materials and structures based on them [1–4]. This method allows us to analyze separately the effect of different components of the equivalent circuit of a semiconductor structure. Therefore, impedance spectroscopy analysis is widely applied for the investigation of semiconductor heterojunctions, which are much more complex compared with homojunctions mainly due to the presence of interface states [5, 6].

In the previous work [7] the detailed quantitative analysis of the impedance of semiconductor heterojunctions was carried out in the presence of series resistance, shunt resistance, parasitic inductance and interface states. The effect of interface states was considered in the scope of the single-level state model [8, 9].

The single-level state model is a first approximation, which cannot be applied for all kind of heterojunctions. Interface traps may create many closely spaced energy levels within band gap that results in an interface state continuum (continuous energy distribution). It is known that

the impedance of a single-level trap differs from that of an interface trap continuum [8–10]. Therefore, in some cases, this fact should be taken into account in order to avoid possible misinterpretations.

The aim of this work is to show quantitatively the effect of interface state continuum on the spectral distribution of the measured impedance and capacitance of semiconductor heterojunctions in comparison with the previous study within the scope of the single-level state model [7].

2. Spectral dependence of impedance

The impedance of semiconductor heterojunctions will be considered in the presence of series, R_s , and shunt, R_{sh} , resistance, parasitic inductance L and interface state continuum in the case of one type (majority) charge carriers' transitions (electrons or holes). The considered equivalent circuit is shown in figure 1.

It is known that the admittance of interface state continuum is given by the following equation [8–10]:

$$Y_s = \frac{qN_{ss}S}{2\tau_m} \ln(1 + \omega^2\tau_m^2) + i\frac{qN_{ss}S}{\tau_m} \arctan(\omega\tau_m), \quad (1)$$

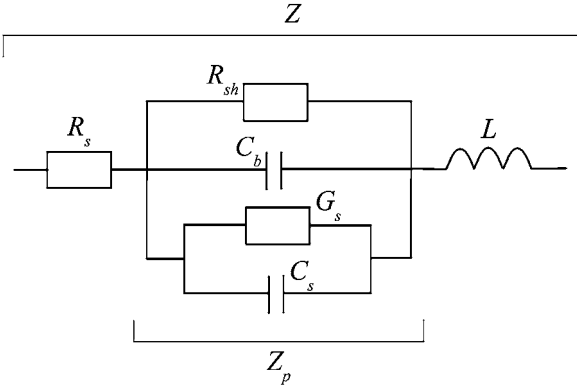


Figure 1. The equivalent circuit of a semiconductor heterojunction in the presence of interface state continuum.

where N_{ss} is interface trap density distribution ($\text{cm}^{-2} \text{eV}^{-1}$), τ_m is characteristic time in the scope of the interface state continuum model, S is the area of a semiconductor heterojunction, q is electron charge, ω is the angular frequency of ac signal. Therefore, the components of the interface state continuum branch: excessive conductance G_s and capacitance C_s are defined by equations (2) and (3), respectively [8]:

$$G_s = \frac{qN_{ss}S}{2\tau_m} \ln(1 + \omega^2\tau_m^2), \quad (2)$$

$$C_s = \frac{qN_{ss}S}{\omega\tau_m} \arctan(\omega\tau_m). \quad (3)$$

It should be noted that equation (1) was derived considering the uniform distribution of the interface state density over a range kT/q near the Fermi level, not over the whole bandgap that is applicable for many real systems [8].

Let us write the expression for the impedance of interface state continuum in order to simplify further calculations;

$$\begin{aligned} Z_s &= \frac{1}{Y_s} = \frac{2\tau_m A}{qN_{ss}S(A^2 + 4B^2)} - i \frac{4\tau_m B}{qN_{ss}S(A^2 + 4B^2)} \\ &= R_0 - i \frac{1}{\omega C_0}, \end{aligned} \quad (4)$$

where

$$A = \ln(1 + \omega^2\tau_m^2), \quad (5)$$

$$B = \arctan(\omega\tau_m), \quad (6)$$

$$R_0 = \frac{2\tau_m A}{qN_{ss}S(A^2 + 4B^2)}, \quad (7)$$

$$C_0 = \frac{qN_{ss}S(A^2 + 4B^2)}{4\omega\tau_m B}. \quad (8)$$

Now the interface state continuum branch (figure 1) can be represented by the series connection of the resistor R_0 and capacitance C_0 . The further analysis of the equivalent circuit can be carried out in the same way as it was done in the previous work [7]. Finally, one can write the expression for the impedance of a semiconductor heterojunction in the presence

of series R_s and shunt R_{sh} resistance, parasitic inductance L and interface state continuum N_{ss} , τ_m :

$$\begin{aligned} Z &= \left[R_s + \left\{ 4\omega\tau_m B \left\{ \frac{\omega\tau_b A}{2B} [qN_{ss}S\tau_b(A^2 + 4B^2) \right. \right. \right. \\ &\quad + 2\tau_m C_b A(1 + \omega^2\tau_b^2)] + \omega^3\tau_b^4 qN_{ss}S \frac{A(A^2 + 4B^2)}{2B} \\ &\quad + 4\omega\tau_m \tau_b C_b B(1 + \omega^2\tau_b^2) \left. \left. \left. \right\} \right\} / \right. \\ &\quad \left. \left\{ \omega^2 [qN_{ss}S\tau_b(A^2 + 4B^2) + 2\tau_m C_b A(1 + \omega^2\tau_b^2)]^2 \right. \right. \\ &\quad + [qN_{ss}S\omega^2\tau_b^2(A^2 + 4B^2) + 4\omega\tau_m C_b B(1 + \omega^2\tau_b^2)]^2 \left. \left. \right\} \right] \\ &\quad + i \left[\omega L - \left\{ 4\omega\tau_m B \left\{ \omega^3\tau_b^2 \left[\frac{qN_{ss}S(A^2 + 4B^2)}{\omega^2} \right. \right. \right. \right. \\ &\quad + \frac{\tau_m C_b A^2}{\omega B} (1 + \omega^2\tau_b^2) \left. \left. \left. \right\} + \omega^3\tau_b^4 qN_{ss}S(A^2 + 4B^2) \right. \right. \\ &\quad + 4\omega^2\tau_b^2 \tau_m C_b B(1 + \omega^2\tau_b^2) \left. \left. \left. \right\} \right\} / \right. \\ &\quad \left. \left\{ \omega^2 [qN_{ss}S\tau_b(A^2 + 4B^2) + 2\tau_m C_b A(1 + \omega^2\tau_b^2)]^2 \right. \right. \\ &\quad + [qN_{ss}S\omega^2\tau_b^2(A^2 + 4B^2) + 4\omega\tau_m C_b B(1 + \omega^2\tau_b^2)]^2 \left. \left. \right\} \right] \\ &= Z' + iZ''. \end{aligned} \quad (9)$$

where $\tau_b = R_{sh}C_b$; A and B are given by equations (5) and (6), respectively; Z' and Z'' are the real and imaginary components, respectively, of the impedance of semiconductor heterojunctions considered in the scope of the interface state continuum model.

The expression for the impedance of semiconductor heterojunctions, analyzed within the single-level state model, was derived in the previous work [7]:

$$\begin{aligned} Z_0 &= \left[R_s + \left\{ \omega^2\tau_b\tau_{ss} [\tau_b qN_{ss}S + \tau_{ss}C_b(1 + \omega^2\tau_b^2)] \right. \right. \\ &\quad + \omega^4\tau_b^4\tau_{ss}qN_{ss}S + \tau_b C_b(1 + \omega^2\tau_b^2) \left. \left. \right\} / \right. \\ &\quad \left. \left\{ \omega^2 [\tau_b qN_{ss}S + \tau_{ss}C_b(1 + \omega^2\tau_b^2)]^2 \right. \right. \\ &\quad + [\omega^2\tau_b^2 qN_{ss}S + C_b(1 + \omega^2\tau_b^2)]^2 \left. \left. \right\} \right] \\ &\quad + i \left[\omega L - \left\{ \omega^3\tau_b^2 \left[\frac{qN_{ss}S}{\omega^2} + \tau_{ss}C_b(1 + \omega^2\tau_b^2) \right] \right. \right. \\ &\quad + \omega^3\tau_b^4 qN_{ss}S + \omega\tau_b^2 C_b(1 + \omega^2\tau_b^2) \left. \left. \right\} / \right. \\ &\quad \left. \left\{ \omega^2 [\tau_b qN_{ss}S + \tau_{ss}C_b(1 + \omega^2\tau_b^2)]^2 \right. \right. \\ &\quad + [\omega^2\tau_b^2 qN_{ss}S + C_b(1 + \omega^2\tau_b^2)]^2 \left. \left. \right\} \right] \\ &= Z'_0 + iZ''_0, \end{aligned} \quad (10)$$

where, $\tau_{ss} = qN_{ss}SR_{ss}$ is the characteristic time of interface states, R_{ss} is the resistance associated with the recharge of interface traps.

Let us simulate spectral dependences given by equations (9) and (10) at the same parameters in order to find out the main differences between the interface state continuum and single-level state models. The theoretically considered parameters are given here: $R_s = 100 \, \Omega$, $R_{sh} = 10^6 \, \Omega$, $C_b = 10^{-10} \, \text{F}$, $N_{ss} = 10^{12} \, \text{cm}^{-2} \text{eV}^{-1}$,

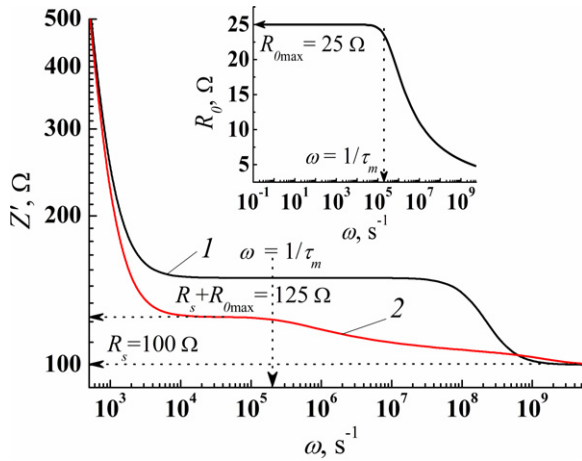


Figure 2. The spectral distribution of the real component of the impedance of the simulated heterojunction: 1—the single-level state model, 2—the interface state continuum model. The inset shows the spectral distribution of R_0 .

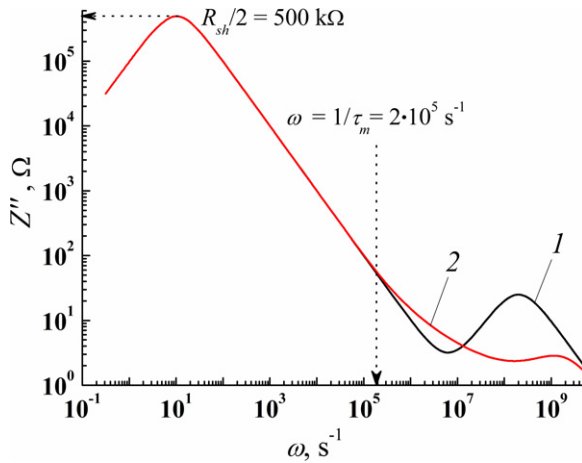


Figure 3. The spectral distribution of the imaginary component of the impedance of the simulated heterojunction: 1—the single-level state model, 2—the interface state continuum model.

$\tau_m = \tau_{ss} = 5 \times 10^{-6}$ s. The parasitic inductance is set to be equal to zero, $L = 0$ H, in order to see the effect of interface states under different conditions at high frequencies.

The comparison of the spectral distributions of the real and imaginary components is shown in figures 2 and 3, respectively. It is seen that the effect of the interface continuum on the real component of the impedance is apparent in the wide frequency range; however, that on the imaginary part is apparent only at $\omega > 1/\tau_m = 2 \times 10^5$ s $^{-1}$.

The saturation of the spectral distribution of the real component Z' , considered in the scope of the interface continuum model (figure 2, curve 2), is interrupted at the frequency $\omega = 1/\tau_m$, as opposite to the single-level state model (figure 2, curve 1). This results from the frequency-dependent parameter R_0 (the inset in figure 2), as opposite to R_{ss} , which is considered to be frequency independent in the context of the single-level state model [7, 8]. It is seen that curve 2 in figure 2 approaches the value that is equal to the series resistance R_s of

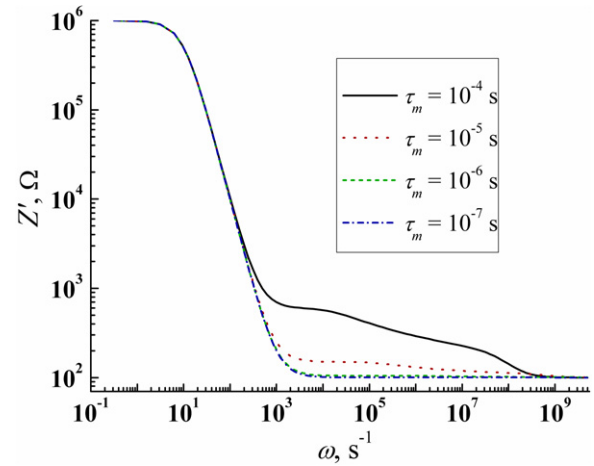


Figure 4. The effect of characteristic time τ_m on the spectral distribution of Z' .

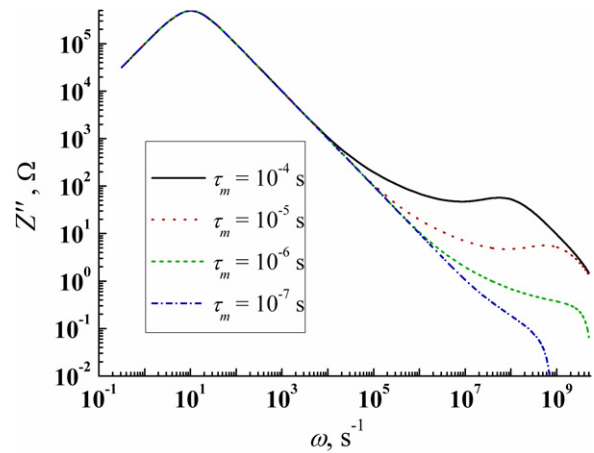


Figure 5. The effect of characteristic time τ_m on the spectral distribution of Z'' .

the simulated heterojunction at a very high frequency of the ac signal.

The spectral dependence of the imaginary component Z'' considered in the scope of the interface state continuum model (curve 2, figure 3) also possesses the second peak. But it is shifted toward higher frequencies and its maximum value is decreased compared to that of the single-level state model (curve 1, figure 3).

Now let us show the effect of interface-states-related parameters τ_m and N_{ss} on the spectral distributions of the real Z' and imaginary Z'' components of the impedance of semiconductor heterojunctions. The previously given parameters will be used for the simulation and $L = 10^{-10}$ H.

It is seen from figures 4–7 that the high frequency features of the spectral distributions Z' and Z'' , second cutoff (real part) and second maximum (imaginary part), disappear with the decrease of τ_m (figures 4 and 5) and with the increase of N_{ss} (figures 6 and 7). The magnitude of the second cutoff and the amplitude of the second maximum are proportional to R_0 in the scope of the interface state continuum model. It is seen that τ_m is in the numerator and N_{ss} is in the denominator of equation (7), which determines R_0 . Therefore, the magnitude of the second cutoff and the amplitude of the second maximum

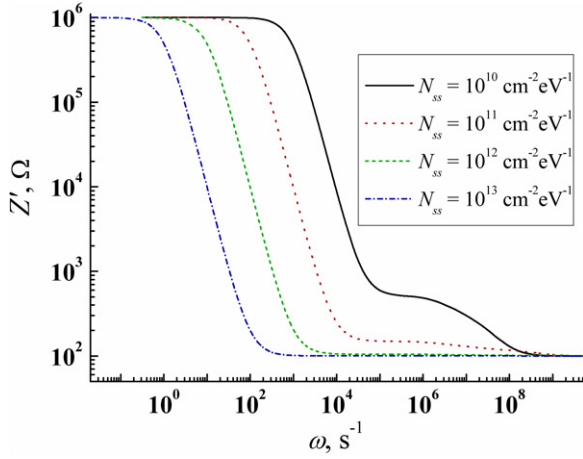


Figure 6. The effect of the interface state density N_{ss} on the spectral distribution of Z' .

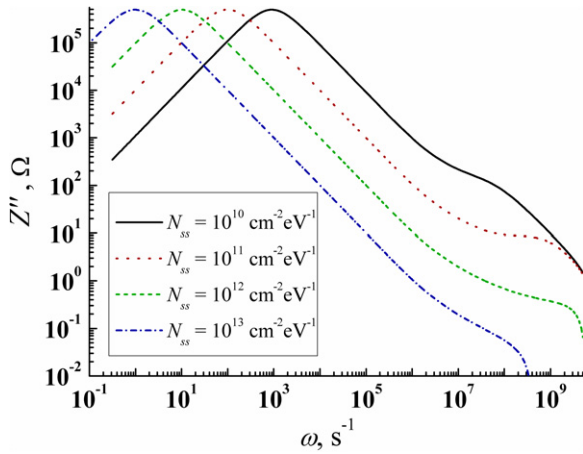


Figure 7. The effect of the interface state density N_{ss} on the spectral distribution of Z'' .

will decrease with the decrease of τ_m and increase of N_{ss} that is shown in figures 4–7.

In the case of small characteristic time τ_m and high interface state density N_{ss} , the impedance spectroscopy of a semiconductor heterojunction, can be wrongly analyzed in the scope of a simple equivalent circuit, which does not take into account the presence of interface states [11–14].

Let us consider the spectral distribution of the real component of impedance Z' . The second cutoff will not be apparent if $R_s \gg R_{0\max}$. Having taken into account the mentioned condition and equation (7), which describes the spectral dependence of R_0 (the inset of figure 2), one can show that the second cutoff of the spectral distribution of Z' will not be observed if the following inequality is true: $\tau_m/N_{ss} \ll qSR_s$ ($A^2 + 4B^2)/2A$ at $0 < \omega < 1/\tau_m$.

One can determine only two parameters, series R_s and shunt R_{sh} resistance, from the spectral dependences of Z' and Z'' plotted in figures 2–7. Therefore, further analysis is needed in order to determine the actual values of interface-state-continuum-related parameters τ_m and N_{ss} and barrier capacitance C_b .

3. Interface-state-continuum-related parameters τ_m and N_{ss}

The admittance of the parallel branch of the equivalent circuit, shown in figure 1, Y_p is given by the following equation:

$$Y_p = \frac{1}{Z_p} = \frac{1}{[Z' - R_s] + i[Z'' - \omega L]} = \frac{[Z' - R_s]}{[Z' - R_s]^2 + [Z'' - \omega L]^2} - i \frac{[Z'' - \omega L]}{[Z' - R_s]^2 + [Z'' - \omega L]^2} = G_p + iB_p, \quad (11)$$

where G_p and B_p are the conductance and the susceptance of the parallel branch, respectively;

$$G_p = \frac{[Z' - R_s]}{[Z' - R_s]^2 + [Z'' - \omega L]^2}, \quad (12)$$

$$B_p = - \left[\frac{[Z'' - \omega L]}{[Z' - R_s]^2 + [Z'' - \omega L]^2} \right]. \quad (13)$$

At the same time the admittance of the parallel branch can be expressed in the terms of τ_m , N_{ss} , R_{sh} and C_b ;

$$Y_p = \left[\frac{qN_{ss}S}{2\tau_m} \ln(1 + \omega^2\tau_m^2) + \frac{1}{R_{sh}} \right] + i \left[\omega C_b + \frac{qN_{ss}S}{\tau_m} \arctan(\omega^2\tau_m^2) \right] = G_p + iB_p, \quad (14)$$

where the G_p and B_p are given by the following equations, respectively:

$$G_p = \frac{qN_{ss}S}{2\tau_m} \ln(1 + \omega^2\tau_m^2) + \frac{1}{R_{sh}}, \quad (15)$$

$$B_p = \omega C_b + \frac{qN_{ss}S}{\tau_m} \arctan(\omega^2\tau_m^2). \quad (16)$$

On the basis of the expressions for the conductance G_p , (12) and (15), we can write the following equation:

$$\frac{1}{\omega} \left[\frac{[Z' - R_s]}{[Z' - R_s]^2 + [Z'' - \omega L]^2} - \frac{1}{R_{sh}} \right] = \frac{qN_{ss}S}{2\omega\tau_m} \ln(1 + \omega^2\tau_m^2). \quad (17)$$

It is seen from equation (17) that the plot of $\{[Z' - R_s]/([Z' - R_s]^2 + [Z'' - \omega L]^2) - 1/R_{sh}\}/\omega$ versus ω possesses the maximum $0.402qN_{ss}S$ at $\omega_0 = 1.977/\tau_m$. Therefore, one can easily determine both interface-state-continuum-related parameters at a fixed external bias;

$$\tau_m = \frac{1.977}{\omega_0}, \quad (18)$$

$$N_{ss} = \frac{\left\{ \frac{1}{\omega} \left[\frac{[Z' - R_s]}{[Z' - R_s]^2 + [Z'' - \omega L]^2} - \frac{1}{R_{sh}} \right] \right\} \Big|_{\max}}{0.402qS}. \quad (19)$$

Figure 8 shows the comparison of the interface-state-related parameters' determination in the scope of the single state model [7] (curve 1) and that in the scope of the interface state continuum model (curve 2) under the following parameters: $R_s = 100 \, \Omega$, $R_{sh} = 10^6 \, \Omega$, $C_b = 10^{-10} \, \text{F}$, $N_{ss} = 6.25 \times 10^{11} \, \text{cm}^{-2} \, \text{eV}^{-1}$, $\tau_m = \tau_{ss} = 5 \times 10^{-6} \, \text{s}$.

If one analyzes the simulated semiconductor heterojunction in the presence of interface state continuum (curve 2 in

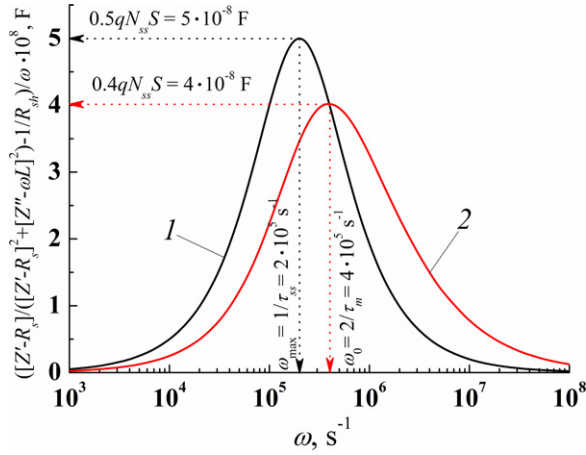


Figure 8. The determination of the interface-trap-related parameters in the scope of: 1—the single-level state model, 2—the interface state continuum model.

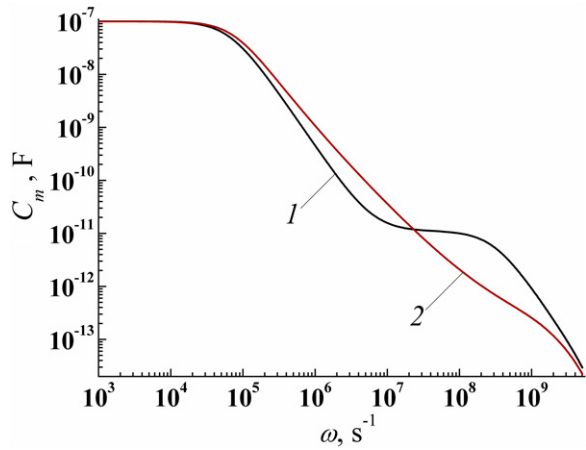


Figure 9. The measured capacitance C_m of the simulated heterojunction ($R_s = 100 \Omega$, $R_{sh} = 10^6 \Omega$, $C_b = 10^{-10} \text{ F}$, $N_{ss} = 6.25 \times 10^{11} \text{ cm}^{-2} \text{ eV}^{-1}$, $\tau_m = \tau_{ss} = 5 \times 10^{-6} \text{ s}$): 1—the single-level state model, 2—the interface state continuum model.

figure 8) in the scope of the single-level state model using equation (20), derived in the previous work [7],

$$\frac{1}{\omega} \left[\frac{[Z' - R_s]}{[Z' - R_s]^2 + [Z'' - \omega L]^2} - \frac{1}{R_{sh}} \right] = \frac{\omega \tau_{ss} q N_{ss} S}{1 + \omega^2 \tau_{ss}^2}, \quad (20)$$

then the interface-state-related parameters will be incorrectly determined. The determined values $\tau_{ss} = 2.5 \times 10^{-6} \text{ s}$ and $N_{ss} = 5 \times 10^{11} \text{ cm}^{-2} \text{ eV}^{-1}$ are not equal to their income values. This fact results in a possible misinterpretation of experimental data during the analysis of semiconductor heterojunctions.

4. Measured and barrier capacitance of semiconductor heterojunctions

The measured capacitance of a semiconductor heterojunction can be expressed in the terms of Z' and Z'' as follows [7]:

$$C_m = \frac{B_m}{\omega} = -\frac{1}{\omega} \left[\frac{Z''}{[Z']^2 + [Z'']^2} \right], \quad (21)$$

where B_m is the measured susceptance.

Figure 9 shows the comparison of the spectral dependences of the measured capacitance considered in the

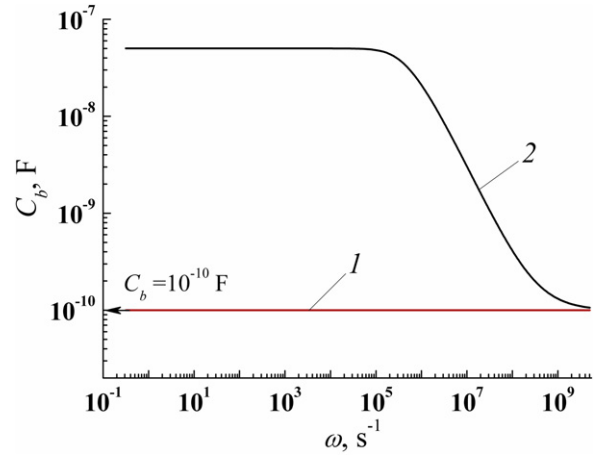


Figure 10. The determination of the actual barrier capacitance C_b of the simulated semiconductor heterojunction in the presence of interface state continuum using: 1—equation (24), 2—equation (25).

scope of single-level state and interface state continuum models under the same parameters.

Both spectral dependences possess similar shapes. At low frequencies, the measured capacitance is equal to the sum of the interface-state-related capacitance and barrier capacitance, $C_m = qN_{ss}S + C_b$.

The decrease of the measured capacitance with the increase of frequency results from the effect of series resistance and parasitic inductance as well as from the decrease of the number of interface states which can follow the high frequency ac signal [7]. However, it is seen that the interface state continuum model provides smoother frequency dependence of the measured capacitance compared to that in the case of the single state model.

Having taken into account the effect of series resistance and parasitic inductance on the spectral dependence of the measured capacitance C_m , the following equation can be written on the base of equations (13) and (16):

$$-\frac{1}{\omega} \left[\frac{[Z'' - \omega L]}{[Z' - R_s]^2 + [Z'' - \omega L]^2} \right] = C_b + \frac{qN_{ss}S}{\omega \tau_m} \arctan(\omega \tau_m). \quad (22)$$

Now let us express $qN_{ss}S$ from equation (17);

$$qN_{ss}S = \frac{2\tau_m}{\ln(1 + \omega^2 \tau_m^2)} \left[\frac{[Z' - R_s]}{[Z' - R_s]^2 + [Z'' - \omega L]^2} - \frac{1}{R_{sh}} \right], \quad (23)$$

and insert into (22). Finally we obtain the formula for the calculation of the actual value of the barrier capacitance C_b in the case of the interface state continuum model;

$$C_b = -\frac{1}{\omega} \left\{ \left[\frac{[Z'' - \omega L]}{[Z' - R_s]^2 + [Z'' - \omega L]^2} \right] - \frac{2 \arctan(\omega \tau_m)}{\ln(1 + \omega^2 \tau_m^2)} \left[\frac{[Z' - R_s]}{[Z' - R_s]^2 + [Z'' - \omega L]^2} - \frac{1}{R_{sh}} \right] \right\}. \quad (24)$$

Formula (24) yields the frequency independent barrier capacitance which is equal to its income value $C_b = 10^{-10} \text{ F}$ (curve 1 in figure 10).

If we calculate the value of the barrier capacitance of the simulated semiconductor heterojunction in the presence of interface state continuum by applying the previously derived equation in the scope of the single state model [7],

$$C_b = -\frac{1}{\omega} \left\{ \left[\frac{[Z'' - \omega L]}{[Z' - R_s]^2 + [Z'' - \omega L]^2} \right] + \frac{1}{\omega \tau_{ss}} \left[\frac{[Z' - R_s]}{[Z' - R_s]^2 + [Z'' - \omega L]^2} - \frac{1}{R_{sh}} \right] \right\}, \quad (25)$$

then the misinterpretation takes place (curve 2 in figure 10), since the calculated value of the barrier capacitance C_b depends on ω that is not physically based within the considered frequency range.

5. Conclusion

The expressions for the spectral dependences of the real and imaginary components of the impedance of semiconductor heterojunctions were derived in the presence of series R_s and shunt R_{sh} resistance, parasitic inductance L and interfaces state continuum τ_m and N_{ss} .

A simulation study of the mentioned spectral dependences was carried out under different values of the interface-state-continuum-related parameters τ_m and N_{ss} . In that study it was shown that in the case of small characteristic time τ_m and high interface state density N_{ss} the impedance spectroscopy of a semiconductor heterojunction can be wrongly analyzed in the scope of a simple equivalent circuit, which does not take into account the effect of interface states (R_s in series with $R_{sh}C_b$ chain). Therefore, the misinterpretation of experimental results is possible.

The approaches for the determination of interface-state-related parameters τ_m , N_{ss} and for the calculation of the actual barrier capacitance C_b were modified in order to take into account the effect of interface state continuum at the heterojunction interface.

It is worth noting that the model discussed in this paper is not better or worse than the model discussed in the previous paper [7]. They are different and each of them can be successfully applied for the analysis of different semiconductor heterojunctions depending on the type of the interface states' system (single-level state or interface state continuum). It is very important to choose the right model in order to avoid possible misinterpretations discussed in this paper. One can use the spectral distribution of the real part of the measured impedance (figure 2) in order to choose the model for further analysis. If the second cutoff is not apparent due to small τ_m or large N_{ss} , one can use equation (24) or (25) in order to distinguish the two models (figure 10).

References

- [1] Barsukov E and Mackonald J R 2005 *Impedance Spectroscopy: Theory, Experiment and Applications* (Hoboken, NJ: Wiley) p 583
- [2] Pautrat J L, Katircioglu B, Mangea N, Bensahel D, Phister J C and Revoil L 1980 *Solid State Electron.* **23** 1159
- [3] Caverly R H and Hiller G 1990 *Solid State Electron.* **33** 1255
- [4] Walter T, Herberholz R, Muller C and Schock H W 1996 *J. Appl. Phys.* **80** 4411
- [5] Oldham W G and Milnes A G 1964 *Solid State Electron.* **7** 153
- [6] Milnes A G and Feucht D L 1972 *Heterojunctions and Metal-Semiconductor Junctions* (New York: Academic) p 408
- [7] Brus V V 2012 *Semicond. Sci. Technol.* **27** 035024
- [8] Nicollan E H and Goetzberger A 1967 *Bell Syst. Tech. J.* **46** 1055
- [9] Sze S M and Kwok K NG 2007 *Physics of Semiconductor Devices* 3rd edn (Hoboken, NJ: Wiley) p 815
- [10] Lehovec K 1966 *Appl. Phys. Lett.* **8** 48
- [11] Berman L S 1972 *Capacitance Methods for Studying Semiconductors* (Leningrad: Nauka) p 104 (in Russian)
- [12] Gol'dberg Yu A, Ivanova O V, L'vova T V and Tsarenkov B V 1983 *Sov. Phys.—Semicond.* **18** 919
- [13] Kavasoglu A S, Kavasoglu N and Oktik S 2008 *Solid State Electron.* **52** 990
- [14] Brus V V 2012 *Semiconductors* **46** 1012